minerals

MDPI

Article

Taphonomic Analysis of the *Sinotubulites* from the Shibantan Member of the Dengying Formation in Yangtze Gorges Area (China)

Xinjie Wang [1], Ben Yang [1,*], Zhihui An [2,*] and Zhongbao Zhao [1]

[1] Institute of Geology, Chinese Academy of Geological Sciences, Beijing 100037, China; yadelohim123@gmail.com (X.W.); zhaozhb04@163.com (Z.Z.)
[2] Hubei Key Laboratory of Paleontology and Geological Environment Evolution, Wuhan Center of China Geological Survey, Wuhan 430205, China
* Correspondence: yangben8@foxmail.com (B.Y.); anzhihui163@163.com (Z.A.)

Abstract: Tubular fossils are a unique metazoan group emerging in the late Ediacaran Period and demonstrating early skeletogenesis and an increase in the diversity of early biocommunities. Among the known records, *Sinotubulites* is widely distributed and distinct in morphology and ultrastructure, holding important evolutionary and stratigraphic significance comparable to the well-known *Cloudina*. However, its biological affinity remains unclear until now. Among various reasons, taphonomic bias is one of the major factors responsible for this, as it not only altered the primary morphology but also modified the ultrastructure and composition of the fossil. Thus, a further study on its taphonomic process would help to decode the biological affinity of *Sinotubulites.* For this purpose, we conducted a taphonomic study on *Sinotubulites* from the top of the Shibantan Member of the Dengying Formation at the Zhongling section in the Yangtze Gorges area (Hubei Province, China). We applied electron backscatter diffraction (EBSD) and cathodoluminescence (CL) to reveal its mineralogical features. EBSD and CL analyses demonstrate that both the fossils and matrix are composed of unoriented calcite, and the matrix shows slight dolomitization with sporadic dolomite grains. The calcite crystals within the *Sinotubulites* tubes are significantly larger than those in the matrix, indicating that the tubular structure provided sufficient space for crystal growth. The absence of lamellar structures in the tubular walls further suggests that the original biogenic material may have been dissolved during diagenetic calcification. The absence of dolomitization in the fossils indicates that this process may have been inhibited by either their large calcite crystals or the enclosed space confined by the outer shell. The identical non-luminescent features of the matrix and fossils suggest that their calcification likely occurred during the same stage. This study demonstrates that taphonomic biases must be accounted for when analyzing the original structure and composition. Additionally, this research documents the occurrence of *Sinotubulites* in the Shibantan Member, representing its lowest stratigraphic horizon in the Yangtze Block.

Keywords: Ediacaran; tubular fossils; EBSD; *Sinotubulites*; Shibantan Member

check for updates

Academic Editors: Olev Vinn and Oluwatoosin Agbaje

Received: 7 April 2025
Revised: 15 May 2025
Accepted: 18 May 2025
Published: 27 May 2025

Citation: Wang, X.; Yang, B.; An, Z.; Zhao, Z. Taphonomic Analysis of the *Sinotubulites* from the Shibantan Member of the Dengying Formation in Yangtze Gorges Area (China). *Minerals* **2025**, *15*, 570. https://doi.org/10.3390/min15060570

Copyright: © 2025 by the authors. Licensee MDPI, Basel, Switzerland. This article is an open access article distributed under the terms and conditions of the Creative Commons Attribution (CC BY) license (https://creativecommons.org/licenses/by/4.0/).

1. Introduction

The Neoproterozoic represents a critical period for the origin and evolution of metazoans. Although molecular studies suggest that multicellular animals originated during the Cryogenian or Tonian [1,2], evidence from body and trace fossils has emerged in the Ediacaran Period [3–8]. Metazoans known in this period are predominantly soft-bodied

organisms [5,9], except for the tubular fossils that developed exoskeletal [10–12]. As the name implies, tubular fossils are a group of millimeter- to centimeter-sized fossils with basically tubulous construction, featuring smooth surfaces or simple ornamentations [10–12]. These fossils are initially found in late Ediacaran strata, with some types extending into the early Cambrian [13].

Ediacaran tubular fossils have been reported globally, including in the Yangtze Block [14–16], Namibia [10], Brazil [17–20], Paraguay [20,21], Laurentia [22,23], Iberia [24], Mongolia [25], and Siberia [26]. Widely distributed in their skeletal properties, Ediacaran tubular fossils show high potential for biostratigraphic applications and play a key role in advancing the subdivision of the Ediacaran System [11,21,27]. Among the records, *Sinotubulites* and *Cloudina* (grouped to cloudinids) are crucial stratigraphic markers of the late Ediacaran and often co-occur in stratigraphic sequences, serving as index fossils for late Ediacaran biozones [21]. However, their phylogenetic affinity has long been debated, with different opinions assigning the representative taxa to cnidarians [28], annelids [10,11,14,25], or algae [29]. These uncertainties mainly stem from their general morphology, ornamentation, and composition while diagenetic processes have often obliterated the limited biological information [21].

Though there was early discovery of cloudinids from Brazil [29], they were initially assigned to Cambrian fossils. The report of *Cloudina from* Namibia confirmed the existence of cloudinids in Precambrian strata. Subsequently, Chen and Wang [30] reported tubular fossils from the Yangtze Block in the Yichang area, Hubei Province. These fossils were tentatively identified as *Cloudina?* sp. based on their resemblance to the initial report of *Cloudina* from Namibia [10]. Later on, these fossils were reclassified to *Sinotubulites baimatuoensis* [14] and reported in other regions of the Yangtze Block [15,16,31–33] as well as United States [34,35], Mexico [36,37], Spain [26], Brazil [21,38] and Namibia [21]. Based on phosphatic specimens of *Sinotubulites* from the Gaojiashan area in southern Shaanxi, studies revealed multilayered tubular walls with abundant irregular folds, smooth inner walls, and longitudinal and transverse ridges on the external surface [32,39]. Given these structural features and their ultrastructural information, researchers have hypothesized that *Sinotubulites* may be analogous to modern biomineralized polychaetes [14,39] and undertake an epibenthic lifestyle [39]. Nevertheless, the observed plastic deformation and ambugous original composition indicates its biomineralization might be dubious [25]. As morphological features have given limited biological information, mineralogical characteristics of *Sinotubulites* become key to decode its phylogenetic affinity [25]. Nevertheless, little attention has been paid to the taphonomic processes of *Sinotubulites* which might have covered and biased the primary structure and composition and thereby inhibit our understanding of its phylogenetic affinity. Under such a context, we carried out a taphonomic study on *Sinotubulites baimatuoensis* discovered from the Shibantan Member of the Dengying Formation at Zhongling, Yichang, Hubei Province. Combining with the traditional technique, i.e., polarizing microscopic and cathode luminescence imaging, we introduce electron backscatter diffraction (EBSD) for in situ mineralogical analyses of the specimens, for the purpose of reveal the mineral properties of the fossil and matrix.

EBSD is a highly precise crystallographic analysis technique primarily applied for the studies of crystal orientation, grain boundaries, and strain states of polycrystalline samples. By detecting Kikuchi patterns formed by the interaction of backscattered electrons with atomic planes on the sample surface, EBSD provides detailed crystallographic information, including crystal structures, unit cell parameters, and crystal orientations [40]. EBSD excels at the high-resolution quantitative characterization of crystal structures on the microscale, making it especially suitable for elucidating crystal texture, nucleation, and growth processes. Thus, EBSD has significant advantages in analyzing the crystallographic information of biominerals.

While applications of EBSD in paleontology are gradually increasing [41–43], its potential for Ediacaran fossil studies remains underexplored. EBSD was selected for this study due to its unparalleled capability to provide high-resolution, quantitative characterizations of microscale crystal structures—critical for distinguishing primary biological signatures from diagenetic overprints, a persistent challenge in the taphonomic analysis of problematic skeletal fossils like *Sinotubulites*. By precisely determining the crystal orientations and mineralogical features of fossils, EBSD clarifies mineral formation mechanisms (e.g., biogenic vs. diagenetic calcification), elucidates crystal growth characteristics (e.g., size, orientation, and spatial distribution), and systematically analyzes taphonomic processes (e.g., dissolution, recrystallization). Cathodoluminescence (CL) was additionally integrated into the analytical framework as its luminescence properties—such as non-luminescent calcite versus sporadically reddish-brown luminescent dolomite—directly reflect diagenetic stages. This enables the timing of the calcification and dolomitization processes to be constrained, complementing EBSD's crystallographic insights by linking mineralogical features to diagenetic histories. Together, these methods enhance the resolution of taphonomic analysis, providing critical evidence to disentangle original biological structures from postmortem alterations, and ultimately explore the phylogenetic affinities of *Sinotubulites*.

2. Geological Background and Research Methods

The Ediacaran Dengying Formation is widely distributed around the periphery of the Huangling Anticline in the Yichang area, Hubei Province, located to the northern margin of the Yangtze Block (Figure 1a). The Dengying Formation on the southern margin of the Huangling Anticline (Figure 1a) has been extensively studied and divided into three members. The basal Hamajing Member is dominated by grayish–white thick-bedded dolostone with teepee structures developed in the upper part. The overlying Shibantan Member consists of dark gray thin-bedded limestone with hummocky cross-stratification. The top Baimatuo Member is dominated by grayish–white thick-bedded dolostone, overlain by the dolostone of the Yanjiahe Formation [44].

The Shibantan Member of the Dengying Formation in the Yichang area, Hubei Province, hosts the Shibantan biota, which is characterized by Ediacara-type and *Yangtziramulus*-type fossils in the lower part, with trace fossils distributed in the lower-middle parts. At the top of the Shibantan Member, *Shaanxilithes ningqiangensis* can occasionally be observed [44]. The newly discovered *Sinotubulites baimatuoensis* samples were collected from the top of the Shibantan Member of the Dengying Formation at the Zhongling section in the eastern Yangtze Gorges area (Figure 1b).

Methods

The specimens (Figure 2) were measured with ImageJ (version 1.54g) to record the length and diameter of the fossils. Subsequently, selected specimens were prepared into thin sections for analysis. The thin sections were then observed under a polarized microscope (Olympus BX51, Olympus Corporation, Tokyo, Japan). Given the stringent requirements of EBSD technology regarding sample surface flatness, conductivity, and stress state, the thin sections underwent multi-stage pretreatments. Initially, the surfaces were finely polished using a Buehler EcoMet300 polisher (Buehler Corporation, Lake Bluff, IL, USA) with 0.3 μm alumina polishing powder or 0.1 μm diamond polishing solution to achieve smoother surfaces. Then, a Buehler VibroMet 2 polisher (Buehler Corporation) was employed for vibratory polishing with a 0.05 μm alumina suspension or a 0.02 μm silica suspension to eliminate surface strain. Finally, the surfaces were coated with ~5 nm carbon films using a Leica EM ACE600 nano-coater (Leica Microsystems, Wetzlar, Germany) to enhance conductivity.

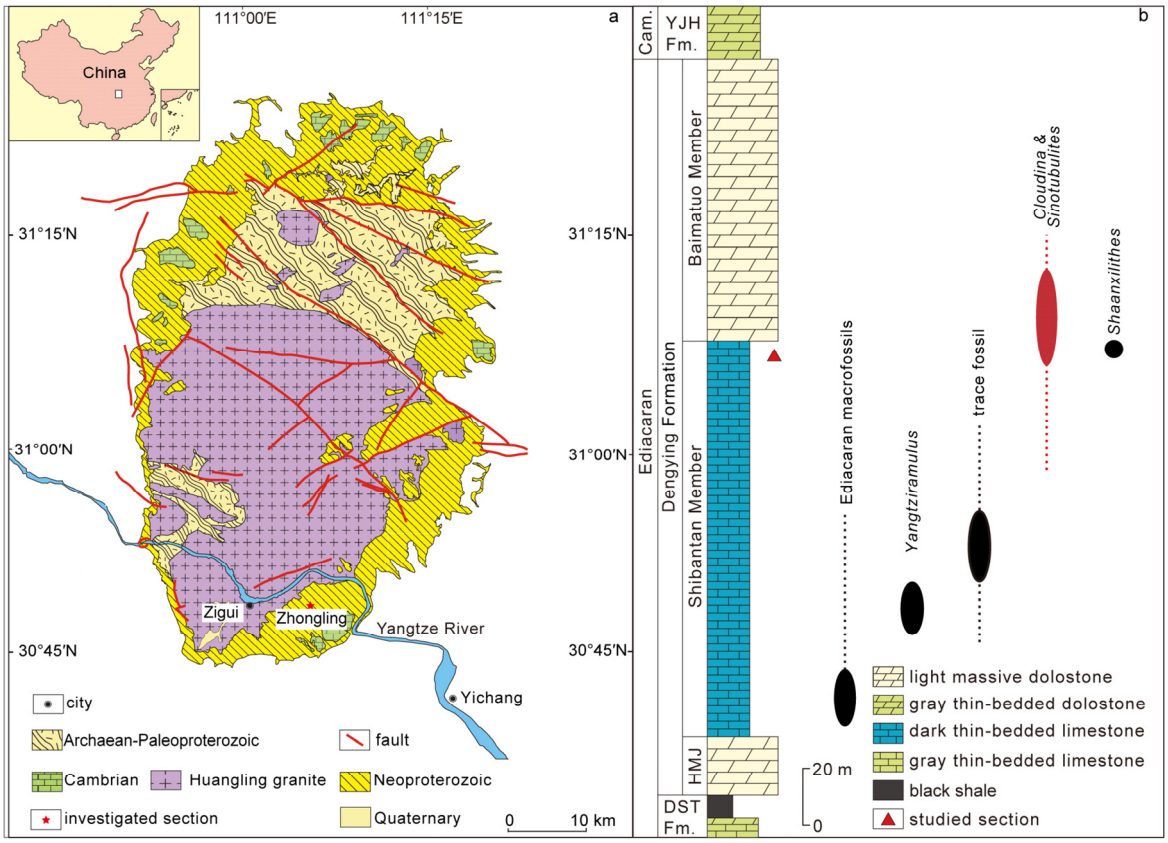


Figure 1. Location and stratigraphic column of the studied section in Huangling Anticline of Yangtze Platform (modified from [44]). (**a**) Location of the Zhongling section in Huangling Anticline. (**b**) stratigraphic column of the Zhongling section, YJH Fm. is short for Yanjiahe Formation. DST Fm. is short for Doushantuo Formation, Camb. is short for Cambrian. Colorful ellipses mark the known distributions of fossils while dashed lines suggest inferred their ranges.

EBSD analysis was subsequently conducted on the thin sections to obtain crystallographic information. During the experiment, measurements were performed using an FEI Quanta450 field emission scanning electron microscope (Thermo Fisher Scientific, Bend, OR, USA), an Oxford Symmetry S3 EBSD high-speed detector (Oxford Instruments, Abingdon, UK), a CMOS high-resolution camera (Oxford Instruments), and an UltimMax energy-dispersive spectrometer (Oxford Instruments). The operating conditions included high vacuum, an accelerating voltage of 20 kV, a current of approximately 130 μA, a tilt angle of 70°, a working distance of 20 mm, and a beam diameter of 6.0 μm. Data acquisition and calibration were performed using the Oxford AztecCrystal software (version 6.1). The pattern resolution was set to 156 × 128 pixels or 622 × 512 pixels, with a gain of 2, and the step size was adjusted between 5 and 10 μm based on the grain size of the sample. The post-processing of the data was also conducted in AztecCrystal, with data quality controlled to ensure a maximum MAD (Mean Angular Deviation) value of 1.0 and grain orientation differences exceeding 10°, ensuring the accuracy and reliability of the results. To facilitate a clearer analysis of the crystals in the fossil wall and internal regions, EBSD data were refined by excluding crystal particles smaller than 100 μm (Figure 3d). Due to the limited presence of dolomite grains in the fossil area (Figure 3b), orientation analysis was performed only on calcite crystals. The calcite grains in the fossil and surrounding matrix were projected onto the {0001}, {1010}, and {1120} planes, and pole density diagrams were generated (Figure 3e,f).

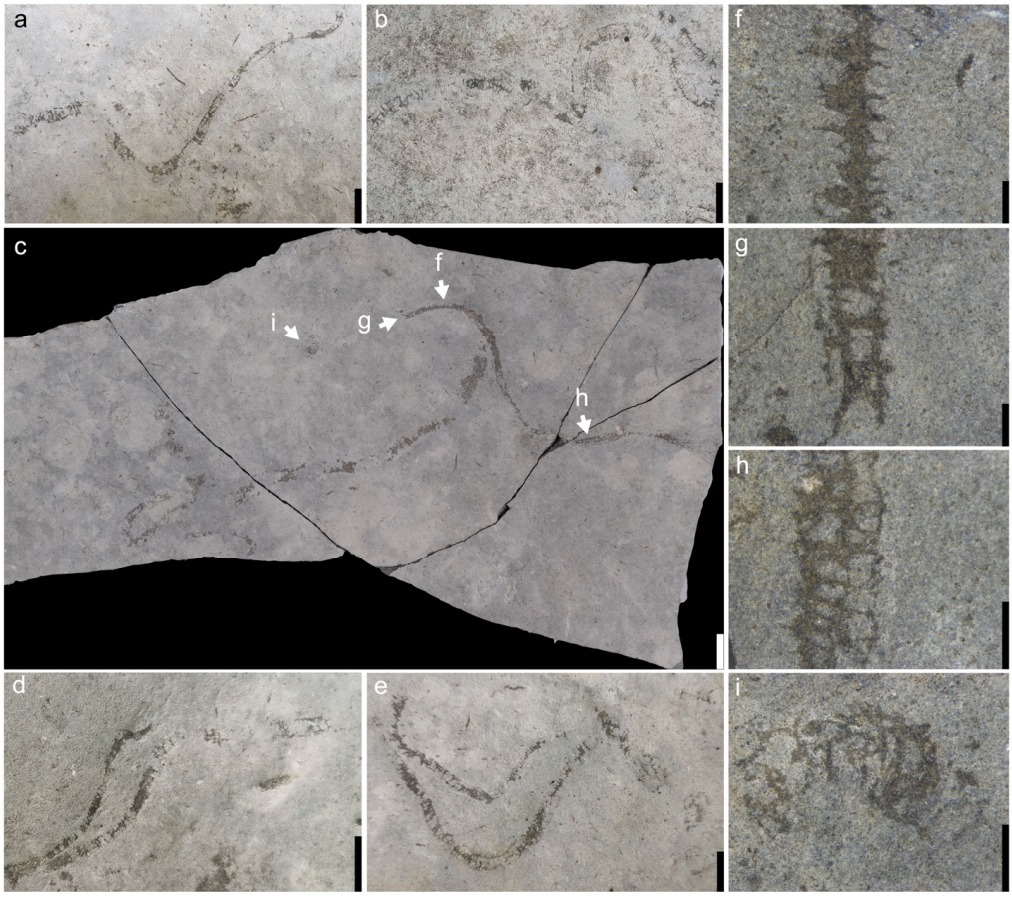


Figure 2. Calcium Carbonatitic *Sinotubulites* from the Shibantan Member of Dengying Formation at the Zhongling section in Huangling Anticline. (**a**) Specimen showing the tubular and curved morphology, sample No. 20ZLAZ021. (**b**) Specimen showing the tubular morphology, sample No. 20ZLAZ022. (**c**) Top view of one hand specimen with two large specimens preserved, sample No. 20ZLAZ001. (**d**) Specimen showing two specimens with tubular and curved morphology, sample No. 20ZLAZ023. (**e**) Specimen showing two specimens with tubular and curved morphology, sample No. 20ZLAZ025. (**f**) Proximal view of (**c**) showing the transverse ridges. (**g**) Proximal view of (**c**) showing the transverse ridges. (**h**) Proximal view of (**c**) showing the transverse ridges. (**i**) Proximal view of (**c**) showing the transverse ridges. Scale: (**c**) is 10 mm, the rest are 1 mm.

Following EBSD analysis, cathodoluminescence (CL) testing was performed using a CL8200-MK5 cathodoluminescence microscope at the College of Earth Science and Engineering, Shandong University of Science and Technology, Qingdao, China. To ensure comparability, the testing conditions were standardized as follows: vacuum at 0.3 Pa, beam voltage at 11 kV, and beam current at 300 μA. Due to the weak luminescence of the samples, the exposure time for imaging was set to 30 s.

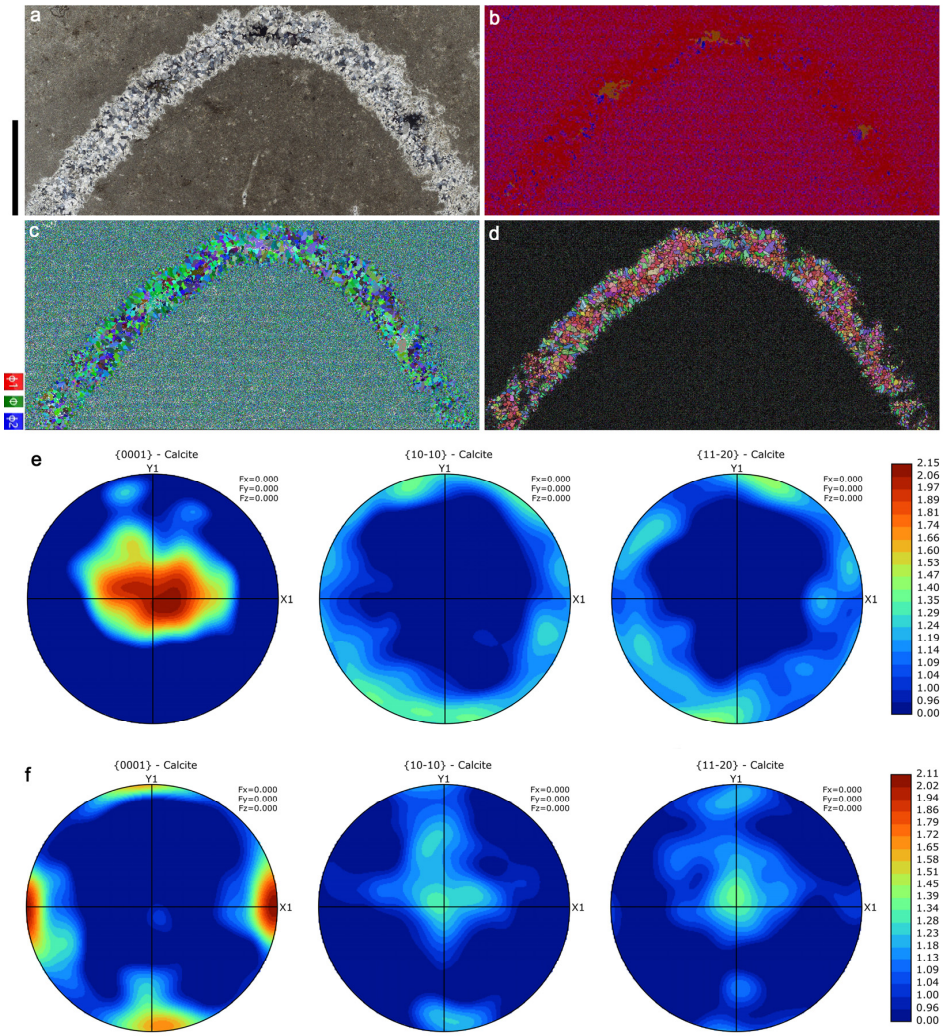


Figure 3. Polarized light image (**a**) and EBSD (**b**–**f**) analysis results of *Sinotubulites* and the matrix sample No. 20ZL002 from the Shibantan Member of the Zhongling section in Huangling Anticline. (**a**) Image of *Sinotubulites baimatuoensis* thin section under a polarized light microscope. (**b**) Composition map obtained from EBSD analysis of the thin section, where red represents calcite, blue-purple represents dolomite, yellow represents quartz, and white indicates components with unidentified crystal structures. (**c**) Crystal phase distribution map with different colors indicating different orientations; large grain boundary parameter set at 10°, and small grain boundary parameter set at 2°. (**d**) Crystal phase distribution map of the fossil region after excluding crystals smaller than 100 μm from (**c**). (**e**) Pole density diagrams for calcite in the fossil region, projected onto the {0001}, {1010}, and {1120} planes. The half-width is set to 20, the projection plane is the XY plane, and the lower hemisphere is selected as the spherical surface. (**f**) Pole density diagrams for calcite in the surrounding matrix, projected onto the {0001}, {1010}, and {1120} planes. Scale bar = 5 mm.

3. Results

Sinotubulites baimatuoensis [14] are preserved in carbonate form (Figure 2) in the top of the Shibantan Member of the Dengying Formation, in the Zhongling section. A total of 45 specimens were collected, with diameters ranging from 1.5 mm to 14.7 mm, and the longest specimen exceeded 22.1 cm in length. Most specimens exhibit a curved or twisted morphology, with transverse and longitudinal ridges on their surfaces.

3.1. EBSD Analysis

Under a polarized light microscope, the interference color of *Sinotubulites baimatuoensis* [14] in the sample 20ZL002 (Figure 3) appears grayish#–white, indicating a carbon-

ate composition (Figure 3a), with minor quartz inclusions (Figure 3a). EBSD analysis (Figure 3b) confirms that the fossil is composed of calcite, while the surrounding matrix consists of a mixture of calcite and dolomite. The crystal phase distribution map (Figure 3c) reveals a disordered arrangement of crystals within the fossil, with no preferred orientation. The crystal grain size in the fossil region is significantly coarser than that in the surrounding rock. The calcite crystals within the fossil exhibit high pole density along the *Z*-axis (Figure 3e), whereas those in the surrounding matrix show well-developed pole density along the X- and Y-axes (Figure 3f). No ordered crystal fabric was observed in the phase distribution map of the fossil region.

The interference color of the sample 20ZL003 (Figure 4) appears grayish–white (Figure 4a). Phase mapping from EBSD analysis (Figure 4b) shows that the fossil and surrounding matrix share consistent carbonate compositions. The fossil is predominantly composed of calcite, while the matrix contains a calcite–dolomite mixture. Calcite crystals within the fossil are euhedral and coarser-grained, yet the crystal phase distribution map (Figure 4c) reveals no preferred crystallographic orientation. Notably, the <0001> axes of the fossil calcite aggregate in 20ZL003 are subparallel to the XY plane, aligning with the matrix calcite fabric.

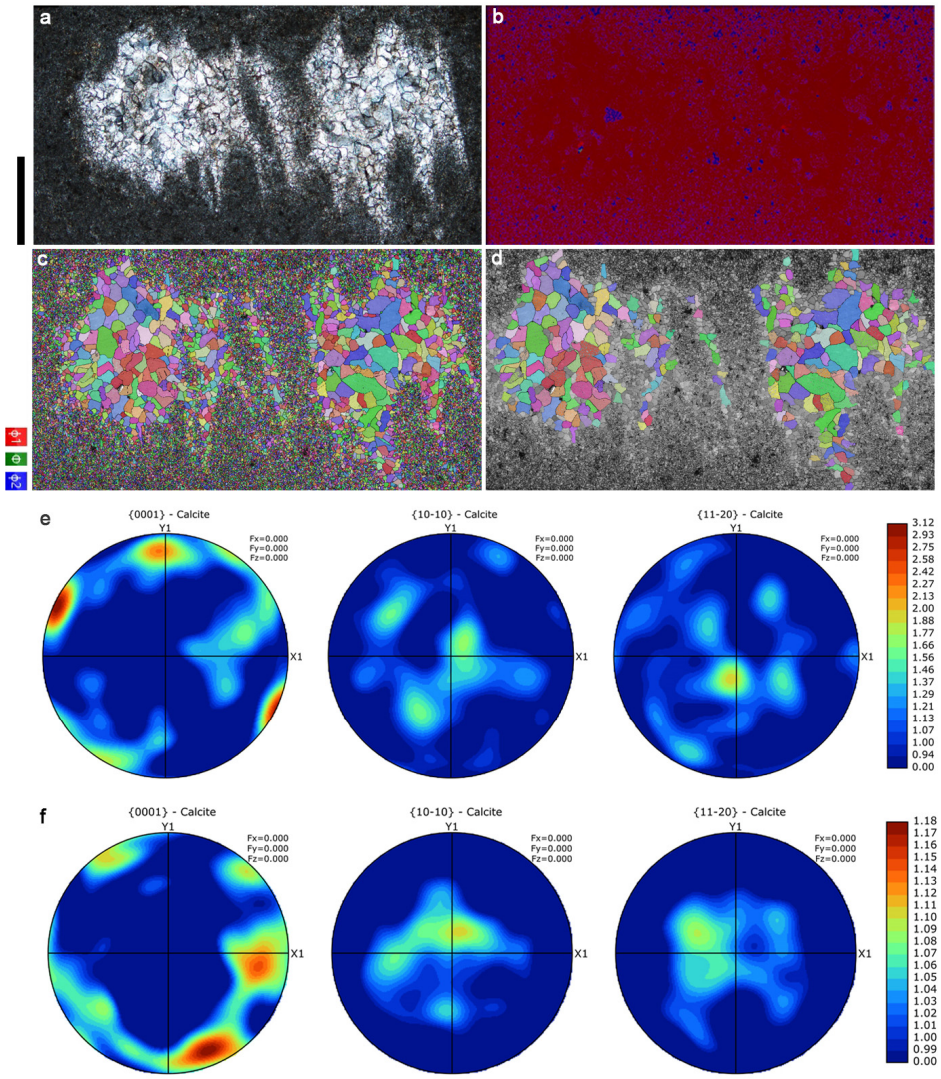


Figure 4. Polarized light image (**a**) and EBSD analysis results (**b**–**f**) of carbonatitic *Sinotubulites* from specimen 20ZL003 from the Shibantan Member of the Zhongling section in Huangling Anticline. (**a**) Polarized

photomicrograph of a rock thin section of *Sinotubulites baimatuoensis*. (**b**) Compositional map derived from the EBSD test of the thin section, in which the red part is calcite, the blue–violet part is dolomite, and the white part is the component with no identified crystal structure. (**c**) Crystal phase distribution map with different colors marking different orientations, where the large grain boundary parameter is 10° and the small grain boundary parameter is 2°. (**d**) Crystallographic phase distribution map containing only crystals from the area where the fossil is located, obtained by excluding crystals smaller than 40 μm in (**c**). (**e**) Polar density maps of calcite {0001}, {1010}, and {1120} facets from the area where the fossil is located, where the half-width is set to 20, the plane of projection is the XY plane, and the chosen spherical plane is the lower hemisphere. (**f**) Pole density maps of the {0001}, {1010}, and {1120} facets of calcite in the enclosing rock region. Scale bar = 5 mm.

3.2. Cathodoluminescence Analysis

The cathodoluminescence (CL) analysis of the two thin sections (20ZL002 and 20ZL003) revealed significant differences in their luminescent features. Most areas showed no distinct luminescence, while fossil regions exhibited complete non-luminescence (Figure 5c,f). CL signals were primarily observed in the surrounding matrix, where luminescent areas appeared reddish–brown with spatially localized, unevenly sized bright spots that contrasted sharply with adjacent non-luminescent domains.

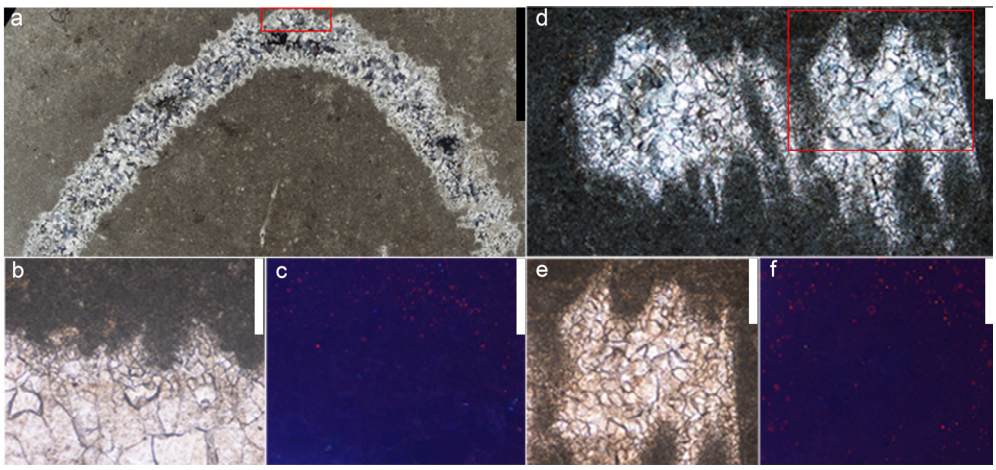


Figure 5. Polarized light (**a**,**b**,**d**,**e**) and cathodoluminescence (**c**,**f**) images of carbonate-preserved *Sinotubulites* specimens from the Shibantan Member at the Zhongling section in Huangling Anticline. (**a**) Polarized light image of thin section 20ZL002 of *Sinotubulites baimatuoensis*. (**b**) Detailed view of the red box in (**a**). (**c**) Cathodoluminescence image corresponding to (**b**). (**d**) Polarized light image of thin section 20ZL003 of *Sinotubulites baimatuoensis*. (**e**) Detailed view of the red box in (**d**). (**f**) Cathodoluminescence image corresponding to e. Scale bars: (**a**) 5 mm; (**b**,**c**,**e**,**f**) 400 μm; (**d**) 500 μm.

4. Discussion

4.1. Taphonomic Implications

Metazoan biomineralization is a process involving the crystallization of minerals within organisms exhibiting ordered orientations [45–49]. While the crystallization texture may be a key condition for assessing the biomineralization in fossil records, attention has rarely been paid to the taphonomic effects that may have modified primary information by dissolution, replacement and recrystallizations during the diagenesis. Consequently, a step-by-step inspection starting from the overall morphological variations to the mineralogical features of the fossils would secure a credible conclusion on the mineralization processes recorded in the fossils.

Previous reports indicate that *Sinotubulites* fossils are usually less than 30 mm in length, with diameters ranging from 0.4 mm to 6 mm (Table 1). The specimens reported here are ten times larger than any previous records. Earlier discoveries of *Sinotubulites baimatuoensis*

may represent fossilized remains formed after the destruction of organismal remains and subsequent diagenesis. The lectotype of *Sinotubulites* shows that the original tubular bodies were decorated with transverse ridges, while corrugations as well as longitudinal ridges were assumed to be secondary features resulting from postmortem compression [21]. Surface corrugations and ridges could be observed in the studied specimens (Figure 2) from the Shibantan Member, indicating that the fossils may have experienced similar compressions and distortion as were observed in the phosphatized specimens of other regions [24,32]. This suggests that such diagenetic deformation is a ubiquitous process among various taphonomic facies (phosphatization and calcification), increasing the suspicion of a highly soft tubular structure of *Sinotubulites*.

Table 1. Measurement of maximum length and diameter of reported *Sinotubulites baimatuoensis*.

Occurrence	Max. Length (mm)	Max. Diameter (mm)	References
Dengying Fm., Yichang, Hubei Prov., China	221.24	14.7	This study
Dengying Fm., Yichang, Hubei Prov., China	18	5	Chen et al., 1981 [14]
Dengying Fm., Shennongjia, Hubei Prov., China	2.8	1	Yang et al., 2020 [15]
Dengying Fm., southern Shaanxi Prov., China	20	4	Chen et al., 2001 [39]
Deep Spring Fm., Mount Dunfee, Nevada, USA	7.6	3.3	Signor et al., 1987 [35]
La Ciénega Fm., Sonora, Mexico	22	2.9	Sour-Tovar et al., 2006 [37]
Villarta Limestone of lbor Group, Bada-joz Prov., Spain	20	6	Cortijo et al., 2015 [24]
Corumbá Group, Mato Grosso do Sul State, Brazil	8	3.1	Hahn and Pflug, 1985 [38]
Mooifontein Member, Nama Group, South Namibia	2.5	0.5	Yang et al., 2022 [21]

Observation reveals that multi-microlayers within tubular walls of the studied *Sinotubulites* are missing (Figures 2–5) and replaced by calcite (Figures 3–5) with the surrounding matrix consisting of a mixture of calcite and dolomite (Figure 5). On the other hand, crystal phase distribution maps of EBSD reveal significant differences in crystal size between the fossil and the surrounding matrix (Figures 3c and 4c). Both crystal orientation distribution maps (Figures 3c,e and 4c,e) and the pole figures (Figures 3e and 4e) show a lack of ordered crystal arrangement in the fossils. These features are likely due to the influence of the microenvironment of the fossil during diagenesis, e.g., its biological structure and organic-rich composition. The tubular coelom may have served as a fluid conduit during the early stage of diagenesis; after the degradation of the soft body as well as the original tubular wall, calcite grew along the tubular wall. Isolated by the tubular structure of *Sinotubulites*, these crystals got enough space for expansion, resulting in large crystals. In contrast, the growth of calcites within the surrounding matrix was restricted by sediments and reached a relatively small size (Figures 3–5). Cathodoluminescence analysis shows that the calcite crystals in both the tubes and the matrix did not luminesce with only sporadic reddish–brown luminescence observed in dolomitic grains. This suggests that a possibly synchronous calcification of the fossil and matrix and a later dolomitization in the matrix while the internal microenvironment of the fossil may have precluded dolomitization within the fossils.

In consideration of the absence of microlayers of the tube walls, as well as the unoriented and nonluminescent calcite of the tube wall, the primary composition of the tube wall of the studied *Sinotubulites* should have been erased during diagenesis. Thus, the determination of whether there was original biomineralization within these specimens

cannot be made. Further studies should be directed toward the specimens with microlayers that may have preserved the original information on biomineralization, if it occurred. Yet, the plastic deformation features, such as bending and twisting, observed in most specimens indicate that *Sinotubulites baimatuoensis* did not exhibit toughness as imparted by a primary structure [25].

4.2. Stratigraphic and Palaeogeographic Implications

Sinotubulites has been identified in the Baimatuo Member [14,15,30,33] in the Yangtze Gorges area. Though initial reports of *Sinotubulites* considered it was from the middle member (Shibantan Member) of the Dengying Formation, the dolostone with chert belts were considered to belong to the overlying Baimatuo Member [44,50]. The discovery of *S. baimatuoensis* in the Shibantan Member provides a new biostratigraphic marker for the stratigraphic correlation of this member, which preserved abundant Ediacaran macrofossils [51,52]. It is worth noting that the boundary between the Shibantan and Baimatuo Members in the Yichang area may exhibit diachronous characteristics, which could explain why tubular fossils have been found at the top of the Shibantan Member or the base of the Baimatuo Member in different sections.

The newly discovered large *Sinotubulites* fossils, characterized by their significant size and excellent preservation, suggest in situ or near-in situ burial. Compared with the thick-bedded dolostones of the Baimatuo Member, the limestones of the Shibantan Member formed in a deeper depositional environment, associated with a shallow marine shelf setting [50]. The low-energy depositional conditions in this region likely provided favorable environments for in situ or near-in situ burial, which facilitated the preservation of these fossils.

5. Conclusions

Sinotubulites from the Shibantan Member of Dengying Formation in Yangtze Gorges area presents missing multilayers in the tube wall and unoriented large calcite crystals with the same luminescent feature as those in the matrix. These factors suggest a strong taphonomic alteration during diagenesis, resulting in the degradation of the biological structure and the missing of primary composition. An assessment of the taphonomic influence is thereby necessary during studies on the biomineralization of *Sinotubulites* and other similar tubular fossils. On the other hand, regardless of the entangling mineralization (biomineralization and diagenesis), the plastic deformation (corrugations, bending and twisting) in the fossils indicates high organic composition of within the original wall of *Sinotubulites*. Of particular significance, this study reports the occurrence of *Sinotubulites* in the Shibantan Member, identifying this as the lowest interval for this genus in the Yangtze Gorges area of Yangtze Block.

Author Contributions: Conceptualization, B.Y.; Methodology, X.W., B.Y. and Z.Z.; Software, X.W. and Z.Z.; Formal analysis, X.W. and B.Y.; Investigation, Z.A., X.W. and B.Y.; Data curation, Z.A.; Writing—original draft, X.W.; Writing—review & editing, B.Y., Z.A. and Z.Z.; Visualization, X.W.; Supervision, B.Y.; Funding acquisition, B.Y. All authors have read and agreed to the published version of the manuscript.

Funding: The study was supported by the Basic Scientific Research Fund of the Institute of Geology, Chinese Academy of Geological Sciences (J2309), National Natural Science Foundation of China (42372042, U2244202), China Geological Survey (DD20230221).

Data Availability Statement: The original contributions presented in this study are included in the article. Further inquiries can be directed to the corresponding authors.

Acknowledgments: We are grateful to the technician XW (Beijing). Comments by five anonymous reviewers improved the manuscript and are greatly acknowledged.

Conflicts of Interest: The authors declare no conflict of interest.

References

1. Dohrmann, M.; Wörheide, G. Dating early animal evolution using phylogenomic data. *Sci. Rep.* **2017**, *7*, 3599. [CrossRef] [PubMed]
2. Dos Reis, M.; Thawornwattana, Y.; Angelis, K.; Telford, M.J.; Donoghue, P.C.J.; Yang, Z. Uncertainty in the Timing of Origin of Animals and the Limits of Precision in Molecular Timescales. *Curr. Biol.* **2015**, *25*, 2939–2950. [CrossRef] [PubMed]
3. Jensen, S. The Proterozoic and Earliest Cambrian Trace Fossil Record; Patterns, Problems and Perspectives. *Integr. Comp. Biol.* **2003**, *43*, 219–228. [CrossRef] [PubMed]
4. Matthews, J.J.; Liu, A.G.; Yang, C.; McIlroy, D.; Levell, B.; Condon, D.J. A Chronostratigraphic Framework for the Rise of the Ediacaran Macrobiota: New Constraints from Mistaken Point Ecological Reserve, Newfoundland. *GSA Bull.* **2020**, *133*, 612–624. [CrossRef]
5. Narbonne, G.M. THE EDIACARA BIOTA: Neoproterozoic Origin of Animals and Their Ecosystems. *Annu. Rev. Earth Planet. Sci.* **2005**, *33*, 421–442. [CrossRef]
6. Fedonkin, M.A.; Gehling, J.G.; Grey, K.; Narbonne, G.M.; Vickers-Rich, P. *The Rise of Animals: Evolution and Diversification of the Kingdom Animalia*; Johns Hopkins University Press: Baltimore, MD, USA, 2007; pp. 1–326.
7. Xiao, S.; Laflamme, M. On the eve of animal radiation: Phylogeny, ecology and evolution of the Ediacara biota. *Trends Ecol. Evol.* **2009**, *24*, 31–40. [CrossRef]
8. Droser, M.L.; Tarhan, L.G.; Gehling, J.G. The Rise of Animals in a Changing Environment: Global Ecological Innovation in the Late Ediacaran. *Annu. Rev. Earth Planet. Sci.* **2017**, *45*, 593–617. [CrossRef]
9. Morris, S.C. The Fossil Record and the Early Evolution of the Metazoa. *Nature* **1993**, *361*, 219–225. [CrossRef]
10. Germs, G. New shelly fossils from Nama Group, South West Africa. *Am. J. Sci.* **1972**, *272*, 752–761. [CrossRef]
11. Hua, H.; Chen, Z.; Yuan, X.; Zhang, L.; Xiao, S. Skeletogenesis and asexual reproduction in the earliest biomineralizing animal *Cloudina*. *Geology* **2005**, *33*, 277–280. [CrossRef]
12. Hua, H.; Cai, Y.P.; Min, X.; Chai, S.; Dai, Q.K. "Tubular animal radiation" at the terminal Ediacaran stage. *J. Northwest Univ.* **2020**, *50*, 141–174, (In Chinese with English Abstract).
13. Yang, B.; Steiner, M.; Zhu, M.; Li, G.; Liu, J.; Liu, P. Transitional Ediacaran–Cambrian small skeletal fossil assemblages from South China and Kazakhstan: Implications for chronostratigraphy and metazoan evolution. *Precambrian Res.* **2016**, *285*, 202–215. [CrossRef]
14. Chen, M.; Chen, Y.; Qian, Y. Some tubular fossils from Sinian–lower Cambrian boundary sequences, Yangtze Gorge. *Bull. Tianjin Inst. Geol. Miner. Resour.* **1981**, *3*, 117–124. (In Chinese)
15. Yang, B.; Shang, X.; Steiner, M.; Liu, P. Ediacaran tubular fossils from the Shennongjia area, Hubei Province, and their stratigraphic significance. *J. Stratigr.* **2020**, *44*, 448–454, (In Chinese with English Abstract).
16. Zhang, L.; Dong, J.; Tian, S.; Ding, L. The Gaojiashan Biota. In *Late Aurignacian–Early Precambrian biota of the northern margin of the Yangzi Plateau*; Ding, L., Zhang, L., Li, Y., Dong, J., Eds.; Science and Technology Literature Press: Beijing, China, 1992; p. 156. (In Chinese)
17. Adorno, R.R.; Walde, D.H.G.; Erdtmann, B.D.; Denezine, M.; Cortijo, I.; Carmo, D.A.D.; Giorgioni, M.; Ramos, M.E.A.F.; Fazio, G. First occurrence of *Cloudina* carinata Cortijo et al., 2010 in South America, Tamengo Formation, Corµmbá Group, upper Ediacaran of Midwestern. *Estud. Geol.* **2019**, *75*, e095. [CrossRef]
18. Walde, D.H.G.; do Carmo, D.A.; Guimarães, E.M.; Vieira, L.C.; Erdtmann, B.-D.; Sanchez, E.A.M.; Adorno, R.R.; Tobias, T.C. New aspects of Neoproterozoic—Cambrian transition in the Corumbá region (state of Mato Grosso do Sul, Brazil). *Ann. Paléontol.* **2015**, *101*, 213–224. [CrossRef]
19. Walde, D.H.-G.; Weber, B.; Erdtmann, B.-D.; Steiner, M. Taphonomy of Corµmbella werneri from the Ediacaran of Brazil: Sinotubulitid tube or conulariid test? *Alcheringa* **2019**, *43*, 335–350. [CrossRef]
20. Warren, L.V.; Quaglio, F.; Simões, M.G.; Gaucher, C.; Riccomini, C.; Poiré, D.G.; Freitas, B.T.; Boggiani, P.C.; Sial, A.N. Cloudina-Corµmbella-Namacalathus association from the Itapucµmi Group, Paraguay: Increasing ecosystem complexity and tiering at the end of the Ediacaran. *Precambrian Res.* **2017**, *298*, 79–87. [CrossRef]
21. Yang, B.; Warren, L.V.; Steiner, M.; Smith, E.F.; Liu, P. Taxonomic revision of Ediacaran tubular fossils: *Cloudina*, *Sinotubulites* and *Conotubus*. *J. Paleontol.* **2022**, *96*, 256–273. [CrossRef]
22. Hagadorn, J.W.; Waggoner, B. Ediacaran fossils from the southwestern Great Basin, United States. *J. Paleontol.* **2000**, *74*, 349–359. [CrossRef]

23. Selly, T.; Schiffbauer, J.D.; Jacquet, S.M.; Smith, E.F.; Nelson, L.L.; Andreasen, B.D.; Huntley, J.W.; Strange, M.A.; O'Neil, G.R.; Thater, C.A. A new cloudinid fossil assemblage from the terminal Ediacaran of Nevada, USA. *J. Syst. Palaeontol.* **2020**, *18*, 357–379. [CrossRef]
24. Cortijo, I.; Martí Mus, M.; Jensen, S.; Palacios, T. Late Ediacaran skeletal body fossil assemblage from the Navalpino anticline, central Spain. *Precambrian Res.* **2015**, *267*, 186–195. [CrossRef]
25. Yang Ben Steiner, M.; Schiffbauer, J.D.; Selly, T.; Wu, X.; Zhang, C.; Liu, P. Ultrastructure of Ediacaran cloudinids suggests diverse taphonomic histories and affinities with non-biomineralized annelids. *Sci. Rep.* **2020**, *10*, 535.
26. Zhuravlev, A.Y.; Liñán, E.; Vintaned, J.A.G.; Debrenne, F.; Fedorov, A.B. New Finds of Skeletal Fossils in the Terminal Neoproterozoic of the Siberian Platform and Spain. *Acta Palaeontol. Pol.* **2012**, *57*, 205–224. [CrossRef]
27. Grant, S. Shell structure and distribution of *Cloudina*, a potential index fossil for the terminal Proterozoic. *Am. J. Sci.* **1990**, *290-A*, 261–294.
28. Vinn, O.; Zaton, M. Inconsistencies in proposed annelid affinities of early biomineralized organism *Cloudina* (Ediacaran): Structural and ontogenetic evidences. *Carnets Géol.* **2012**, *3*, 39–47. [CrossRef]
29. Beurlen, K.; Sommer, F.W. Observações estratigráficas e paleontológicas sôbre o calcário Corumbá. *Bol. Geol. Mineral.—DNPM* **1957**, *168*, 1–47.
30. Chen, M.; Wang, Y. Note on the tubular metazoan fossils from the Dengying Formation of the upper Sinian System in the Gorge District of the Yangtze River. *Chin. Sci. Bull.* **1977**, *22*, 219–221. (In Chinese)
31. Hua, H.; Zhang, L.; Zhang, Z.; Wang, J. New fossil evidences from latest Neoproterozoic Gaojiashan biota, South Shaanxi. *J. Paleontol.* **2000**, *39*, 381–390. (In Chinese)
32. Cai, Y.; Xiao, S.; Hua, H.; Yuan, X. New material of the biomineralizing tubular fossil *Sinotubulites* from the late Ediacaran Dengying Formation, South China. *Precambrian Res.* **2015**, *261*, 12–24. [CrossRef]
33. Liang, D.; Cai, Y.; Nolan, M.; Xiao, S. The terminal Ediacaran tubular fossil *Cloudina* in the Yangtze Gorges area of South China. *Precambrian Res.* **2020**, *351*, 105931. [CrossRef]
34. Signor, P.W.; McMenamin, M.A.S.; Gevirtzman, D.A.; Mount, J.F. Two new pretrilobite faunas from western North America. *Nature* **1983**, *303*, 415–418. [CrossRef]
35. Signor, P.W.; Mount, J.F.; Onken, B.R. A pre-trilobite shelly fauna from the White–Inyo region of eastern California and western Nevada. *J. Paleontol.* **1987**, *61*, 425–438. [CrossRef]
36. McMenamin, M.A.S. Basal Cambrian small shelly fossils from the La Ciénega Formation, northwestern Sonora, Mexico. *J. Paleontol.* **1985**, *59*, 1414–1425.
37. Sour-Tovar, F.; Hagadorn, J.W.; Huitrón-Rubio, T. Ediacaran and Cambrian index fossils from Sonora, Mexico. *Palaeontology* **2007**, *50*, 169–175. [CrossRef]
38. Hahn, G.; Pflug, H.D. Die Cloudinidae n. fam., KallRöhren aus dem Vendium und Unter-Kambrium. *Senckenberg. Lethaea* **1985**, *65*, 413–431.
39. Chen, Z.; Sun, W. Late Simian (tubular) metazoan fossils: *Cloudina* and *Sinotubulites* from southern Shaanxi. *Microb. Palaeontol. Lett.* **2001**, *18*, 180–193, 199–202.
40. Doddapaneni, S.; Kumar, S.; Sharma, S.; Shankar, G.; Shettar, M.; Kumar, N.; Aroor, G.; Ahmad, S.M. Advancements in EBSD Techniques: A Comprehensive Review on Characterization of Composites and Metals, Sample Preparation, and Operational Parameters. *J. Compos. Sci.* **2025**, *9*, 132. [CrossRef]
41. Zhu, X.; Wang, Q.; Wang, X. Electron backscatter diffraction (EBSD) study of elongatoolithid eggs from China with microstructural and parataxonomic implications. *Paleobiology* **2024**, *50*, 330–345. [CrossRef]
42. Cusack, M. Biomineral electron backscatter diffraction for palaeontology. *Palaeontology* **2016**, *59*, 171–179. [CrossRef]
43. Grenier, C.; Berent, K.; Rodríguez-Navarro, A.; Vinn, O.; Checa, A.G. Microstructures, crystallography and growth patterns of serpulid tubeworms (Class Polychaeta). *Mar. Biol.* **2024**, *171*, 231. [CrossRef]
44. An, Z.H.; Ye, Q.; Tong, J.N.; Tian, L.; Zhao, X. Stratigraphic Sequence of the Ediacaran Dengying Formation around the Huangling Anticline, Western Hubei Province: Implications for Regional Stratigraphic Correlation. *Earth Sci.* **2024**, *49*, 2992–3009, (In Chinese with English Abstract).
45. Skinner, H.C.W.; Jahren, A.H. Biomineralization. *Treatise Geochem.* **2003**, *8*, 682.
46. Levi-Kalisman, Y.; Falini, G.; Addadi, L.; Weiner, S. Structure of the nacreous organic matrix of a bivalve mollusk shell examined in the hydrated state using cryo-TEM. *J. Struct. Biol.* **2001**, *135*, 8–17. [CrossRef]
47. Lowenstam, H.A.; Weiner, S. *On Biomineralization*; Oxford University Press: New York, NY, USA, 1989; ISBN 978-0-19-504977-0.
48. Marin, F.; Luquet, G.; Marie, B.; Medakovic, D. Marin2007. In *Current Topics in Developmental Biology*; Elsevier: Amsterdam, The Netherlands, 2007; Volume 80, pp. 209–276. ISBN 978-0-12-373914-8.
49. Nudelman, F.; Sommerdijk, N.A.J.M. Biomineralization as an Inspiration for Materials Chemistry. *Angew. Chem. Int. Ed.* **2012**, *51*, 6582–6596. [CrossRef]

50. Zhao, C.; Zeng, X.; Li, X.; Zhen, J.; Zhou, P.; Gui, K.; Zhang, H. A discussion on the sedimentary environment of Shibantan Member of Dengying Formation in the eastern Yangtze Gorges area. *Geol. China* **2013**, *40*, 1129–1139. (In Chinese)
51. Chen, Z.; Zhou, C.; Xiao, S.; Wang, W.; Guan, C.; Hua, H.; Yuan, X. New Ediacara fossils preserved in marine limestone and their ecological implications. *Sci. Rep.* **2014**, *4*, 4180. [CrossRef]
52. Chen, Z.; Zhou, C.; Yuan, X.; Xiao, S. Death march of a segmented and trilobate bilaterian elucidates early animal evolution. *Nature* **2019**, *573*, 412–415. [CrossRef]

Disclaimer/Publisher's Note: The statements, opinions and data contained in all publications are solely those of the individual author(s) and contributor(s) and not of MDPI and/or the editor(s). MDPI and/or the editor(s) disclaim responsibility for any injury to people or property resulting from any ideas, methods, instructions or products referred to in the content.